Induced seismicity in a salt mine environment evaluated by a coupled continuum-discrete modelling

Diego Mercerat, Mountaka Souley, Lynda Driad-Lebeau, Pascal Bernard

INDUCED SEISMICITY IN A SALT MINE ENVIRONMENT EVALUATED BY A COUPLED CONTINUUM-DISCRETE MODELLING.

MERCERAT Diego[1], SOULEY Mountaka[2] , DRIAD Lynda[2] , BERNARD Pascal[3]

[1] LAEGO – Parc de Saurupt, Ecole des Mines de Nancy, 54000 Nancy cedex, France; diego.mercerat@mines.inpl-nancy.fr

[2] INERIS – Parc de Saurupt, Ecole des Mines de Nancy, 54000 Nancy cedex, France; Mountaka.Souley@ineris.fr, Lynda.Driad@ineris.fr

[3] Laboratoire de Sismologie - IPGP, 4 Place Jussieu, 75005 Paris cedex, France; bernard@ipgp.jussieu.fr,

ABSTRACT: With the objective to better understand the induced microseismicity in a salt mine environment due to an underground solution mining, an in situ experiment is undertaken by GISOS[1] in the Lorraine salt basin. The overburden overlying the salt cavity is characterized by the presence of two competent layers where most microseismic events are expected. This paper presents a coupled continuum-discrete modelling to simulate the mechanics of fracture initiation and propagation in the rock mass overlying the cavity: discrete approach for the competent layers and continuum approach for marls, salt and other rocks and soils. For the competent layers, numerous calibrations of the model microparameters based on the laboratory results are firstly performed. The first coupled modelling results suggest that the mechanism of fracturing in the competent layers is predominantly tensile as it could be expected. The results also show that the microseismic events associated to the progressive damage in the competent layers through microcraks development can be modelled. This opens interesting perspectives to assess the feasibility of seismic monitoring of underground cavities by comparing, in the future, the numerical modelling results with the recorded seismicity of the study area.

KEYWORDS: Induced seismicity, salt cavity, competent layer, in situ, continuum-discrete modelling, , microcraks,

RESUME : Dans l'objectif de mieux comprendre la microsismicité induite dans des mines de sel, une expérimentation in situ a été entreprise par le GISOS sur une cavité saline de la région Lorraine. Le recouvrement est caractérisé par la présence de deux bancs raides dans lesquels l'essentiel de l'activité microsismique est attendue lors de la reprise de l'exploitation. Ce papier présente une modélisation basée sur une approche couplée : continue (pour les marnes et le sel) et discrète (pour les bancs raides) pour évaluer les mécanismes de développement des fractures dans le recouvrement. De nombreuses calibrations des microparamètres du modèle discret à partir des paramètres macroscopiques ont été nécessaires. Les résultats de la modélisation montrent que le mécanisme de fracturation dans les bancs compétents résulte essentiellement d'efforts en traction. Les premiers résultats montrent aussi que les évènements microsismiques peuvent très bien être mesurés à travers la formation des microfissures. Ceci ouvre des perspectives intéressantes pour des confrontations avec les mesures qui seront enregistrées lors de l'effondrement provoqué.

MOTS-CLEFS :: Sismicité induite, cavité saline, banc raide, in situ, modélisation continue-discrete, microfissures

---

[1] GISOS (Groupement de recherche sur l'Impact et la Sécurité des Ouvrages Souterrains) réunissant l'INPL, le BRGM, l'INERIS et l'Ecole des Mines de Paris

1. Introduction

A research project within the GISOS program has been launched in order to assess the feasibility of seismic monitoring of underground growing cavities due to salt dissolution (solution mining). Within such framework, this specific project focus on two main complementary axes : (a) the validation of induced seismicity monitoring techniques in salt mine environments, and (b) the numerical modelling of deformation and failure mechanisms with their associated acoustic emissions as well as the induced microseismicity.

Previous studies on induced seismicity of underground growing cavities (Johnston and Einstein 1990, Mendecki et *al.* 1999) confirm the presence of microseismic events associated with the progressive damage of the overburden until its final collapse. Continuous monitoring of such microseismicity may provide crucial information for stability analysis of the area surrounding the cavity. In order to validate such seismic monitoring techniques, a microseismic network has been installed over a site test at Cerville-Buissoncourt (Lorraine, France), where a stable brine cavity is nowadays found. When the salt exploitation restarts, the spatial and temporal evolution of the seismic event locations can firstly be recorded and secondly be correlated with the results of mechanical modelling.

Numerical modelling of such complex process requires a large scale model which takes into account both the cavity evolution within the salt layer and the mechanical behaviour of the overburden layers where high deformation and fracturing are expected. To achieve this scientific challenge (experimental and numerical through geophysics and geomechanics fields), a coupled continuum and discrete modelling strategy is then adopted.

This paper focus on the feasibility to achieve the previous scientific objective and presents the preliminary numerical results of induced microseismicity evolution in the competent layers through the microcracks distribution.

From numerical point of view and in order to take into account the elasto-brittle behaviour of the competent layers where most seismic damage is really expected, we use the code PFC2D (Particle Flow Code in two dimensions) based on the discrete element method. To describe the behaviour of the other layers (mainly composed of marls and salt) which present more ductile and/or viscoplastic behaviour, a continuum approach based on the bidimensional Fast Lagrangian Analysis of Continua code (FLAC) is used allowing for different and more complex constitutive laws.

Numerous calibration process are firstly performed to estimate the microparameters used in PFC2D to reproduce the macroscopic stress-strain curves obtained from laboratory tests (macroscopic behaviour from uniaxial and triaxial tests).

A large scale continuum model assuming an elastic perfectly plastic behaviour of the competent layers is firstly built in order to establish the suitable boundary conditions with regard to the brine cavity sizes. Finally, a fully coupled continuum-discrete model is developed (coupling between FLAC and PFC2D domains is achieved through a special function written in the internal language of both codes), as well as a comparison with the previous continuum approach.

2. Site test of Cerville-Buissoncourt

2.1. *Brine cavity and overburden characteristics*

The brine cavity of Cerville-Buissoncourt (Lorraine, France) is actually located within a salt layer at about 180 m depth and it presents an irregular shape but in a first approximation, it can be

considered as a cylindrical cavity of 100 m of diameter and 50 m high. An schematic geological section of the study area is shown in Figure 1. Typically, the overburden is characterized by the presence of a series of intercalated anhydritic marls lying over the salt layer, and on top of them, the presence of two competent layers of 8.5 m thickness with an elasto-brittle behaviour located approximately 50 m above the salt layer. These layers correspond to what is known as the Beaumont dolomite (a dolomite of 5 m thick and an anhydrite of 3.5 m thick).

2.2. *Microseismic network*

A microseismic network has been installed over the underground brine filled cavity of Cerville-Buissoncourt. The network includes four 3D components and three 1D component seismometers located at different depths in cemented boreholes distributed around the study area. A velocity model of the area, from the processing of a 2D seismic line (work in progress), will allow us to obtain an accurate location of microseismic events when the salt exploitation restarts . The spatial and temporal evolution of the seismic event locations can then be correlated with mechanical modelling results, and therefore a quantitative analysis of seismic and non-seismic deformation will be available.
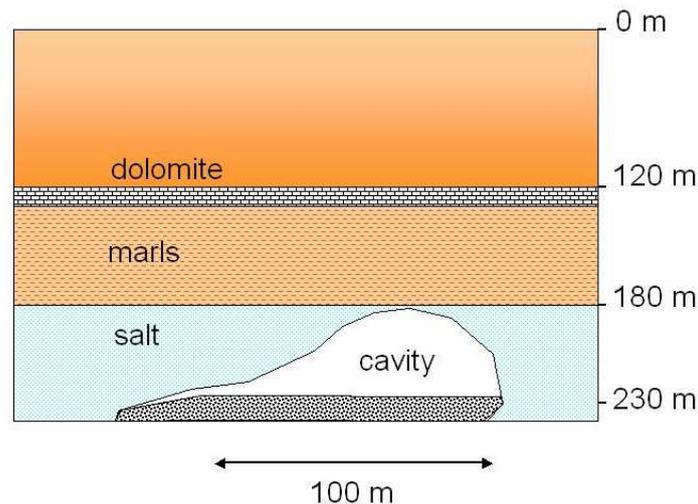

Figure 1. Schematic section of the salt cavity and main geological facies.

3. Geomechanical laboratory characterization

A large number of laboratory tests have been carried out on SOLVAY S.A samples to characterize the geological formations of interest. Some of them are available (by courtesy) for this study. In particular, the Beaumont dolomite and the anhydrite facies present a rather high Young modulus (~80 GPa) and uniaxial compressive strength (UCS ~200 MPa) for typical sedimentary rocks. The tensile strength measured by Brazilian tests is also high. The acoustic properties of these competent layers are quite elevated.

On the other hand, the mean values found for samples extracted from the marls located between the salt layer and the Beaumont dolomite are much lower, with extremely low tensile strengths measured in some samples.

The results of this geomechanical laboratory characterization are used to choose the physical and mechanical parameters of the numerical model, and to obtain the appropriate microproperties, by means of a calibration process that will characterize the PFC2D inclusion within the continuum. For

numerical modelling purposes, we do not differentiate between the two competent layers (Beaumont dolomite and anhydrite facies).

4.   Modelling strategy

4.1.   Philosophy and coupling continuum-discrete modelling

When the salt exploitation restarts, the cavity will progressively grow leading to develop irreversible damage within the upper layers until the final collapse. Numerical modelling of such a complex process requires a large scale model which takes into account both the cavity evolution within the salt layer and the mechanical behaviour of the overburden layers where high deformation and fracturing are expected.

From previous mechanical laboratory investigations, both competent layers exhibit a clear elastic and brittle behaviour. To keep the elasto-brittle behaviour of the competent layers where most of seismic damage is expected and in order to directly compare the acoustic emission (AE) events, we use the PFC2D code. That allows us to represent the damage within the competent layers directly by the formation and tracking of microcracks. A detailed description of the PFC2D model and the theory is provided elsewhere (see for example Hazzard et al. 2000 ; Potyondy and Cundall 2004). Below we briefly present the main characteristics of this code.

To describe the behaviour of the other layers (mainly consisted of marls and salt) which present more ductile and/or viscoplastic behaviour, a continuum approach based on the code FLAC (a 2 dimensional finite difference code widely used by the scientific and industrial communities) is employed. This leads to approach more complex rheological behaviours based on continuum mechanics (elastoplastic with or without hardening and softening, viscoelastic or viscoplastic). Hence, the brittle layers are modelled in PFC2D as an inclusion of bonded circular particles embedded in a classical FLAC grid, the applied forces received from PFC2D act on the grid points along the inclusion boundary. The translational velocities of these boundary particles are received from FLAC. The full coupling between FLAC and PFC2D boundaries is achieved through a special function written in the internal *FISH* language.

4.2.   Short description of PFC2D code

The PFC2D code models the rock mass as an assembly of particles bonded together to reproduce cohesion. The bond that connects two neighboring particles can break apart if the normal or shear stress at the bond exceeds its normal or shear strength, respectively. This corresponds to the explicit formation of a microcrack, with the spontaneous generation of a stress wave that can propagate outward from the crack. Therefore, PFC2D was extensively used to model acoustic emission in rock specimens (Hazzard and Young, 2002, 2002b) and to simulate fault zones (Hazzard et al., 2002). Interesting studies were conducted to associate many cracks that occur very close in space and time, into one microseismic event of spatial dimension of several broken bonds (Hazzard and Young, 2002b). This allows to explicitly assign seismic source parameters, such as moment tensor or magnitude values, emergent from the modelled material that can be compare with those obtained from observations.

However, in our numerical simulations, not all zones in the numerical model are necessarily submitted to large stress variations and exhibit contact breaks. Apart from that, despite the extensive use of PFC to model elasto-brittle failure in rock and some other interesting progress (Dedecker et al., 2004), it is not clear at the present time how to model more complex rheological

behaviours in PFC2D. Only the competent layers overhanging the salt cavity will be modelled with this code.

4.3. PFC2D microproperties calibration

In PFC2D, the particle contact stiffness, the contact coefficient of friction and the contact bond model between different particles govern the mechanical behaviour of the material. These are known as the microparameters (or microproperties) of the bonded particle model. They must be chosen in order to reproduce the relevant material properties measured in the laboratory tests (at a macroscale) of the rock specimen to be modelled. This calibration process is not specified a priori and a trial-and-error procedure is generally used. Nevertheless there is some knowledge and guidance based on previous research on PFC2D calibration (Kulatilake et al. 2001; Potyondy and Cundall, 2004) about the relation between each microparameter and its effect on mechanical properties (Table 1).

Following this guidance and using the previous laboratory results, we have calibrated our discrete model of the Beaumont dolomite by simulating a Brazilian test and three biaxial compression tests (at 0.1, 2 and 5 MPa of confining pressure). We used a parallel bonded model material because it seems to well approximate the mechanical behaviour of a brittle elastic cement joining two bonded particles.

This calibration process is firstly performed on the more realistic particle arrangement; say a random packing arrangements around a mean grain size. However, when the specimens are created using a random packing of particles, an extra effort is needed to obtain a uniform stress state within the sample with low 'locked-in' stresses, and to eliminate 'floaters' (particles with less than three contacts with neighbouring particles). For this reason, the calibration process is also performed on a regular hexagonal packing of particles. Some differences in the microparameters and tensile-shear microcrack initiation thresholds are therefore to be expected, particularly for microcrack densities which are dependent on the porosity of the particle packing arrangement.

Table 1. Relations between microparameters and mechanical properties.

Microproperties	Macro mechanical property
Normal (k_n) and shear (k_s) contact stiffness	Young's modulus (E) and Poisson's ratio (ν)
Normal (σc) and shear (τc) bond strengths	Uniaxial Compression Strength (UCS)
Friction coefficient (μ) – Particle clustering Ratio shear/normal bond strength	Slope of failure envelope
Mean bond strength (σc) – Particle radius	Brazilian strength (σ_t)

4.3.1 Random packing

We have firstly verified the independence of the mechanical properties to the mean particle radius by performing ten different biaxial test simulations with similar microproperties. For each mean particle radius, we only change the random number generator. As expected, when increasing the resolution (increasing the number of particles along the shortest dimension of the model), the coefficient of variation (ratio of standard deviation to mean) of each material property decreases as

it was confirmed by Potyondy and Cundall (2004). From these tests, the retained microparameters are given in Table 2 and the emergent macroproperties are shown in Table 3.

Table 2. Model microproperties for the competent layers samples (parallel bonded model). Random packing.

Particles	Cement
$\rho = 2820$ kg/m^3	$\underline{E}_c = 65$ GPa
$D_{max}/D_{min} = 1.5$ $D_{avg} = 0.5$ cm (D: particle diameter)	$\underline{k}_n/\underline{k}_s = 2.5$
$E_c = k_n/2 = 65$ GPa	$\underline{\sigma}c = 120 \pm 60$ MPa
$k_n/k_s = 2.5$ $\mu = 0.5$	$\underline{\tau}c = 240 \pm 60$ MPa

Table 3. Macroproperties of the PFC2D model of the competent layers samples (80 x 160 mm^2 specimens).

Property	PFC2D model $\mathbf{D_{avg} = 0.5}$ cm (number of samples = 10)
E (GPa)	78.3 ± 2.4
ν	0.261 ± 0.031
UCS (MPa)	173.2 ± 8.6
ϕ (deg)	42 ± 4
c (MPa)	37.9 ± 5.1
σ_t (MPa)	44.1 ± 4.5

4.3.2   Regular hexagonal packing

The calibration of a regular hexagonal packing model was carried out starting from the retained values of the previous model shown in Table 2 for Davg (average particle diameter) of 0.5 cm. This regular arrangement of particles allows a straightforward installation of a required uniform stress within the sample by slightly modifying the particle radius. This may be useful for later applications regarding the coupling with FLAC code.

As expected, the stiffness and unconfined compressive strength of a regular packing specimen are much higher than those corresponding to a random packing specimen. For this reason, in order to keep an identical response, we drastically decrease both the bond strengths and stiffnesses of the regular hexagonal model (compare Tables 2 and 4). Similar behaviour in terms of independence of microparameters with particle radius and upscaling to regional dimensions are obtained. In Table 4 we show the retained microparameters for the hexagonal packing bonded particle model that reproduce the mean elasto-brittle behaviour of the Beaumont dolomite.

Finally, Figure 2(a) compares the simulations of uniaxial test with random and regular particle packing and the observed ones. Figure 2(b) illustrates the development of microcracks at different stage of axial stress (pre-peak corresponds to 50% of peak; peak and post-peak related to the end of test).

Table 4. Model microproperties for the competent layer samples. Hexagonal packing.

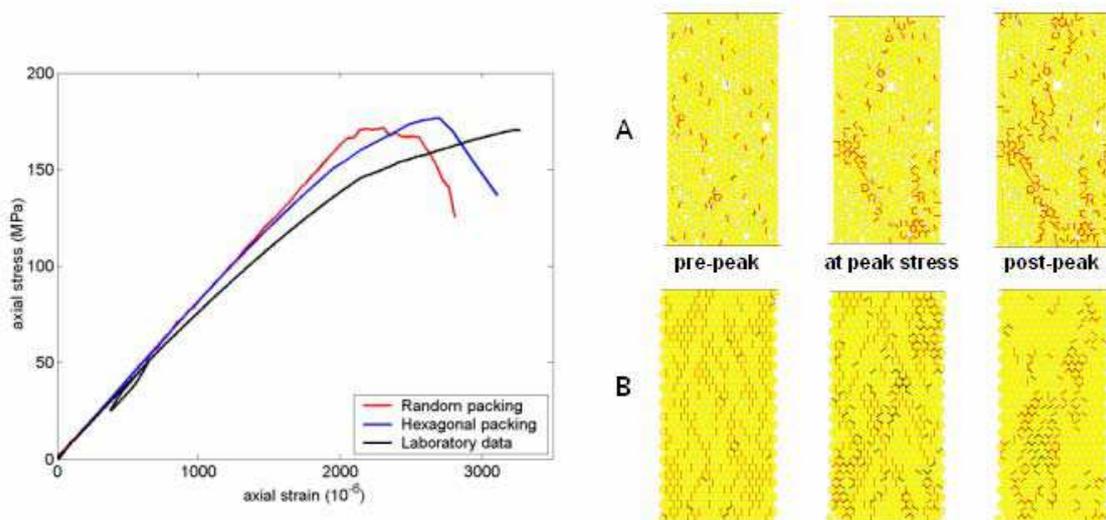| Particles	Cement
$\rho = 2820$ kg/m^3	$E_c = 30$ GPa
$D = 0.5$ cm	$k_n/k_s = 2.5$
$E_c = k_n/2 = 30$ GPa	$\sigma c = 25 \pm 10$ MPa
$k_n/k_s = 2.5 \quad \mu = 0.5$	$\tau c = 50 \pm 10$ MPa

Figure 2. Uniaxial compressive test : (a) Example of axial stress-strain curve for regular and random packing and the experimental curve, (b) Microcracks distribution (A random packing, B regular hexagonal packing) at three different stages of axial stress (tensile cracks in red, shear cracks in black)

4.4. Geomechanical model

The geometrical model shown in Figure 3 is essentially composed of :

- the salt formation extending from the bottom boundary of the model up to the actual brine cavity roof,

- on top of the salt layer, a formation of intercalated marls composed of thin anhydritic to clayley marls with relatively weak mechanical characteristics,

- and the overburden characterized by two competent layers (dolomite and anhydrite level), followed by a series of carbonates, sandstones and marls layers up to the surface.

The geomechanical characteristics of the salt, the competent layers and the intercalated marls are known from the laboratory tests whereas the characteristics of the other materials are inspired on the literature of these basins. For the PFC2D inclusion (in the coupled scheme) we use the microproperties previously calibrated. The inclusion is also represented in the model.
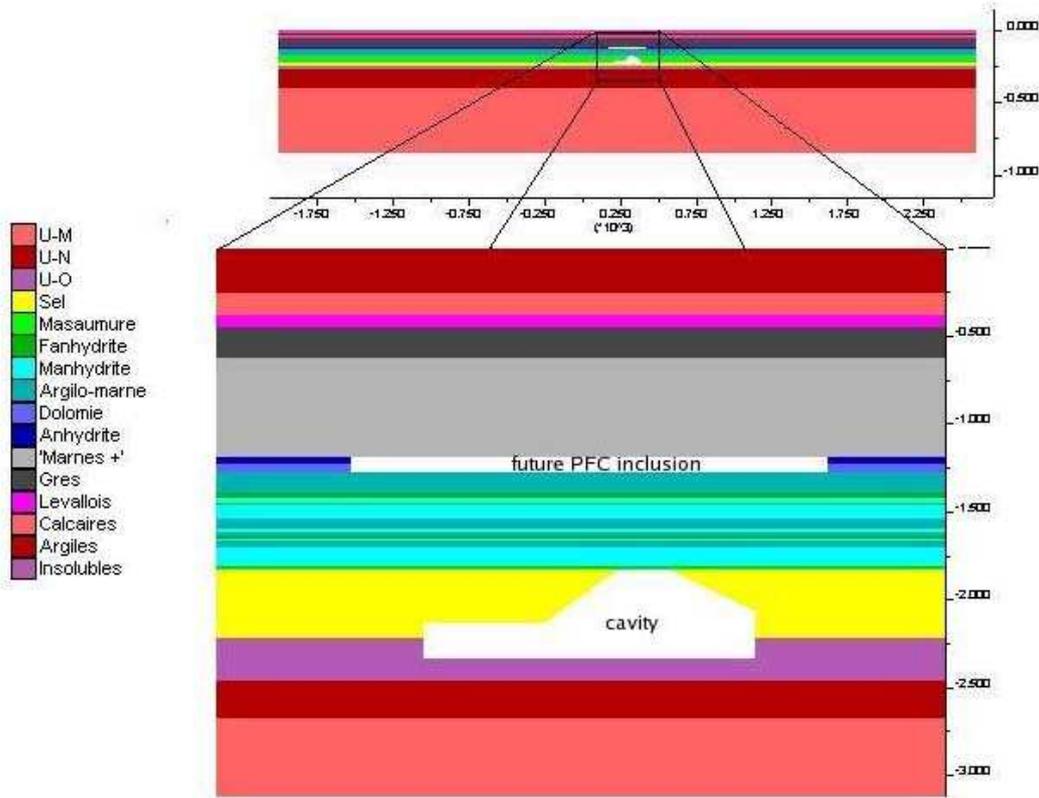

Figure 3 – Detail of the geomechanical model used in this study: the cavity in the salt layer and the PFC inclusion (used later in the coupled scheme) within the competent layers are shown.

In a first time and in order to calibrate the boundary conditions, many simulations have been carried out using an elasto-plastic behaviour for the competent layers, the corresponding optimal geomechanical model is then used in this study. The final geometrical model is 4600 m large and 850 m high.

Because of the absence of symmetry of the cavity, the problem is thus three-dimensional. In spite of its three-dimensional nature and for reasons of simplicity, we chose to perform our analysis in 2D for these first calculations. While considering a section in the greatest dimension of the cavity, we place ourselves in conditions of plane deformations. Consequently, the boundary conditions are:

- no vertical displacement at the bottom boundary of the model (assumption of fixed substratum).

- no horizontal displacement at the lateral boundaries (they are placed far enough to neglect any influence from the cavity filling out process).

The initial stress state is assumed to be isotropic: this assumption is well justified within the salt layer where null initial deviatoric stress is expected. In absence of data concerning the initial stresses in the other materials, we also admit that they are isotropic (a sensitive analysis on the stress anisotropy ratio in such formations can be undertaken on the basis of the literature data). Finally, the vertical stress is equal to the overburden weight.

The initial conditions within the PFC inclusion and in the cavity before the exploitation restarts:

- we established an unifrom isotropic stress of 3 MPa within the PFC domain corresponding to the approximate initial stress found at the inclusion depth due to the overburden weight .

- When the cavity is full of brine, a normal stress acting on the cavity walls equal to $\lambda \, \sigma_0$ is imposed (σ_0 is the overburden weight at the corresponding depth, and $\lambda=0.5$). The progressive filling out of the cavity is modelled by progressively reducing λ from 0.5 to 0 (empty state of the cavity).

5.   Results of large scale modelling

5.1. *Fully continuum approach*

As previously mentioned in the continuum approach, we assume that all off the competent layers are viewed as an elastoplastic material. The aim of this assumption is: (a) to guarantee the type of boundary conditions (applied forces or fixed normal displacements) that will be specified, as well as the external model dimensions with regard to the cavity size, and (b) to keep the model reaction (global response under the initial conditions and when filling out the cavity).

The vertical displacement evolution on top of the Beaumont dolomite and the subsidence at the topography surface are illustrated in Figure 4 as a function of the brine pressure within the cavity: (a) $\lambda = 1$ virgin rock mass, (b) $\lambda = 0.5$ initial state of the cavity full of brine, (c) $\lambda < 0.5$ simulating a progressive filling out of the cavity ($\lambda = 0$ representing the empty state of cavity).
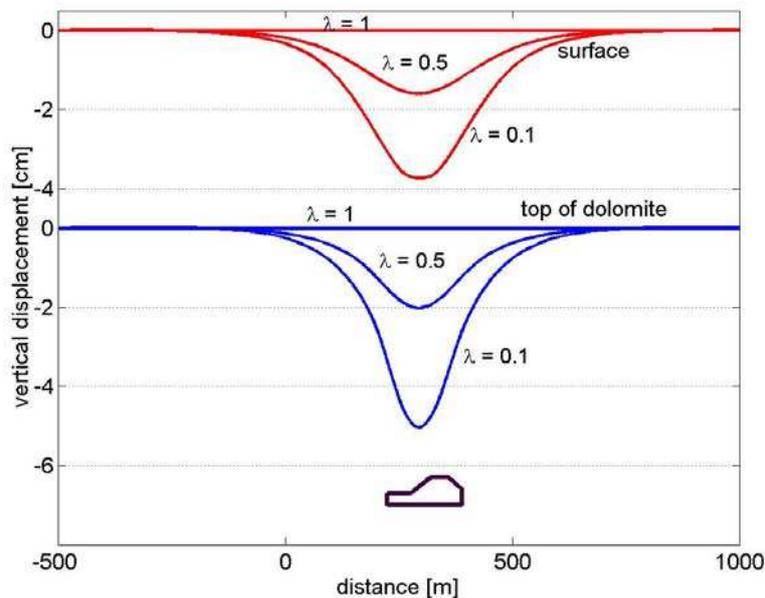

Figure 4. Vertical displacement evolution at the surface and at the top of dolomite (the salt cavity is schematically shown).

In Figure 5, we can appreciate the state of the plastic zones through the layers lying on top of the cavity for λ around of 0.1. The competent layers remain stable and the plasticity migrates from the weakest layers within the intercalated marls and located at the immediate roof, up to the base of the

competent layers. For $\lambda = 0$, most rock materials intercalated between the salt formation and the dolomite fail, leading to a significant stress report in the competent beds.
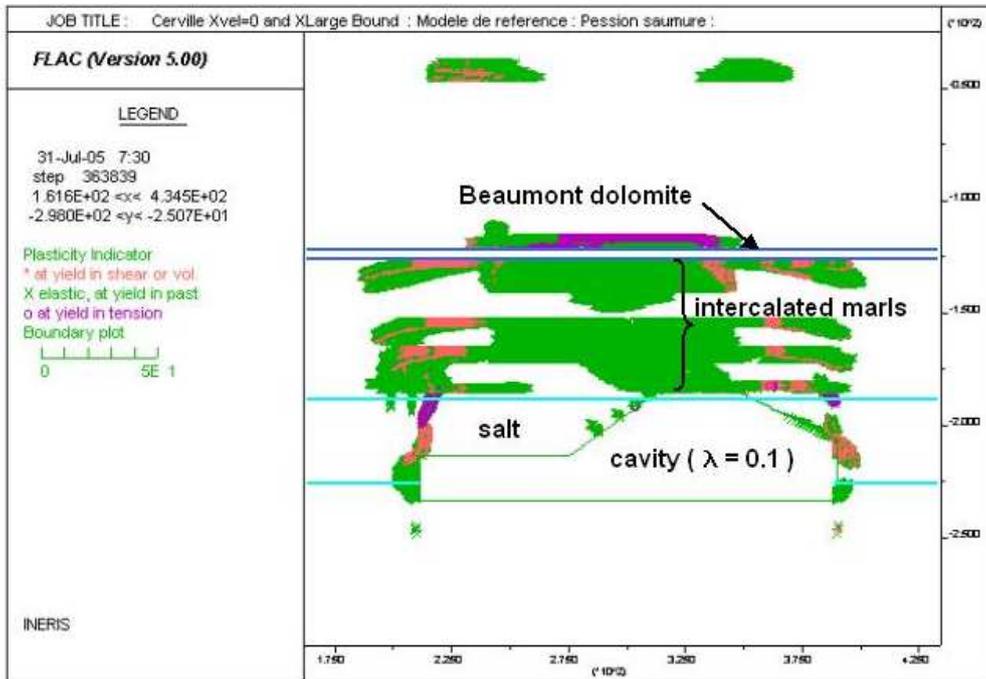

Figure 5. State of plasticity in the overburden layers for λ = 0.1. The competent layers remain stable (without plastic points).

5.2. *Coupled continuum-discrete approach*

The coupling scheme embeds a PFC2D inclusion region within the FLAC grid (the complementary domain of the inclusion in the competent beds where microseismic events are not expected is modelled as a continuum domain). A PFC2D material must be created to confirm the inclusion region such that a single layer of particles overlaps the boundary as illustrated in Figure 6. The applied forces received from PFC2D act on the grid points along the inclusion boundary. The translational velocities of these boundary particles are received from FLAC after one step of calculation (*i.e.* after the motion calculation where velocities and displacements are computed based on the internal and external forces acting on the gridpoints).

Using the calibrated hexagonal parallel bonded model[2], a rectangular PFC2D inclusion within the FLAC model has been created. As a first step, we decided to limit the inclusion to the region where the greatest variation in ambient stress are produced due to the cavity growing. The inclusion centred on top of the actual cavity, is 260 m long by 8.5 m thick, and it covers the dolomite and the anhydrite levels (see Figure 3). Filling this area with circular particles of 0.5 m diameter gives a total number of 10800 particles forming the inclusion. A detail of the coupled model can be seen in Figure 6.

Before establishing the coupling process, a uniform isotropic compressive stress of 3 MPa is obtained within the PFC2D inclusion prior to its connection to the FLAC grid. This allows faster convergence of the initial coupled model to be stabilized. For the rest, the coupled FLAC-PFC2D

---

2 Due to difficulties encountered in installing an initial stress state near 3 MPa with a random particle packing, we have use for this feasibility study the regular particle packing, some differences are therefore to be expected.

scheme is run with similar boundary and initial conditions as the fully FLAC simulations specified in the previous section.
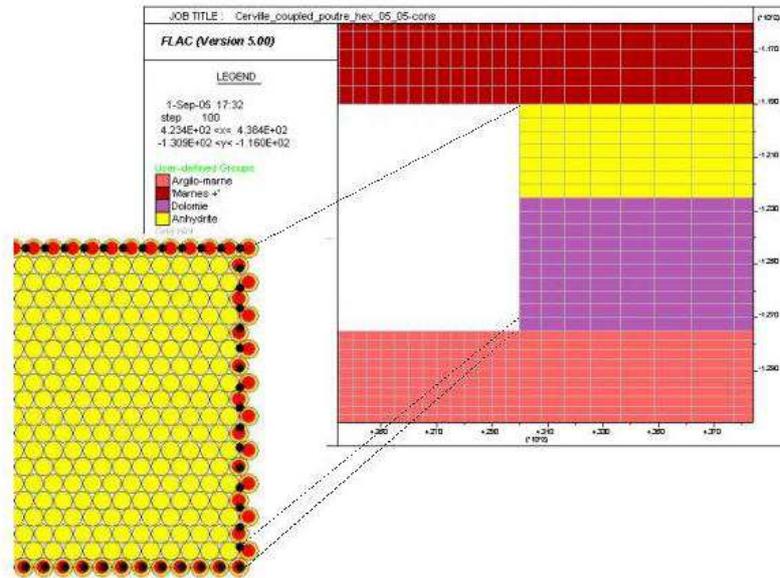

Figure 6. Detail of the right limit of PFC2D inclusion within the FLAC grid. Boundary particles (red) and grid node positions (black) are shown in the PFC2D domain.

The resulting force distribution in the cement between particles of the PFC inclusion can be seen in Figure 7. From $\lambda = 0.5$ down , we can appreciate the increasing zone in tension at the middle of the inclusion, where almost all microcraking occurs. A number of tensile cracks develop first with a random spatial distribution and concentrating later in the central part of the inclusion (just on top of the cavity). The number of microcraks (also shown in Figure 7) increases from about 20 at $\lambda = 0.5$, up to more than 100 at $\lambda = 0.1$. There is a sudden rise up between $\lambda = 0.3$ and $\lambda = 0.1$ manifesting the failure instability within the stiff layer. However, a clear tensile fracture can not be identified at this stage, as it was the case for the fully continuum modelling approach (see Figure 5).
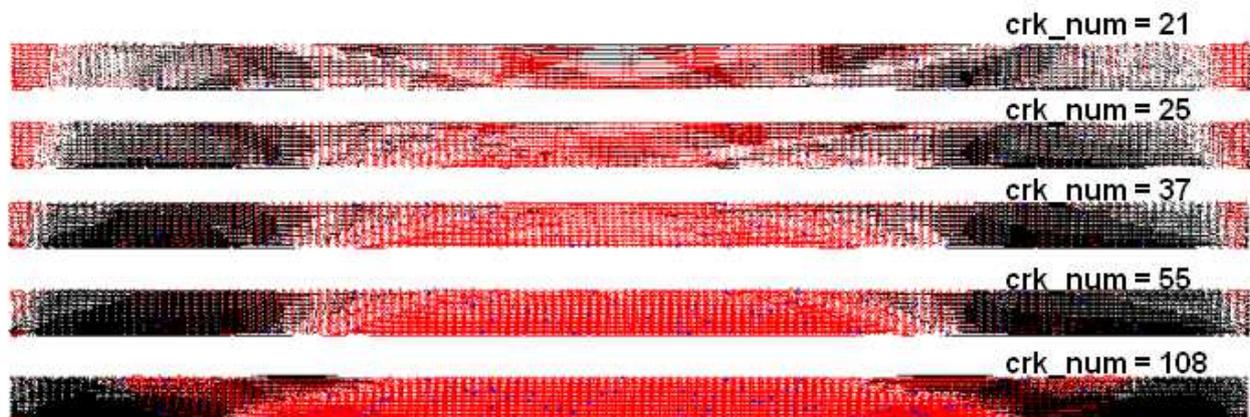

Figure 7. Bond forces in the cement between particles (black = compression, red = in tension) of the PFC inclusion at (from top to bottom) λ = 0.5, 0.4, 0.3, 0.2 and 0.1. Tensile cracks are shown in blue.

6. Concluding remarks

We have presented a preliminary investigation of a coupled continuum-discrete modelling strategy to analyse a complex geomechanical and geophysical process in a salt mine-environment. This involves the fracturing and deformation of the overburden due to brine pumping out and the consequent pressure decrease in the underground cavity.

Based on the results of a laboratory geomechanical characterization, we have calibrated the microproperties of the PFC2D model to be used as the discrete inclusion within the competent layers in the overburden. We used both a random and hexagonal particle packings to create the parallel bonded specimens. The influence of the particle size and the scale effect was analysed. We do not notice any drastic change in the emergent mechanical properties of the modelled materials at both the laboratory and regional scale. This suggests that the use of PFC for modelling the elaso-brittle behaviour of competent layers at the regional scale should be satisfactory.

On the other hand, the effect of particle packing seems to be extremely important in the macro response of the modelled material. The samples created with an hexagonal regular packing are stiffer than those created with a random packing. Also the former present much higher compressive and tensile strengths while keeping the same microproperties for both specimen types. That forced us to perform another calibration process of microparameters for this form of particle packing.

We obtained the first results with the coupled FLAC-PFC2D scheme using an hexagonal PFC2D inclusion 260 m length by 8.5 m height embedded in the Beaumont dolomite layer. The development of microcracking is in accordance with the predicted tensile zone obtained with a fully continuum approach. On the other hand, the sudden rise up of the microcracks number can be interpreted as the damage initiation within the competent beds. A conclusive statement about the failure mechanisms could be achieved when information about real microseismic event locations will be available.

Let us notice that this work is a preliminary one in such complex geomechanical modelling field. In addition, the presented results remain specific to several simplified assumptions taken compared to reality; in particular for the cavity geometry and its evolution, but also for the geomechanical properties of certain materials at the immediate roof and in the overburden, which influence the behaviour of the competent layers.

This research opens many new perspectives in modelling the induced seismicity of the study area. The following steps should be: (a) after installation of the initial stress state in the PFC2D inclusion by assuming a more realistic particle packing (random packing), to perform a sensitive analysis on the microcrack threshold, and evaluate its effect on the mechanism of microcrack growth, while computing the associated AE; (b) to compare these numerical modelling results with those of the measurements recorded in situ after restarting of salt exploitation in a few months.

7. References

Cundall P. A., Strack O (1979). *A discrete element model for granular assembies.* Geotechnique, 29, 47-65.

Dedecker F., Billaux D. *Evaluation of damage-induced permeability in the bure site using a three dimensional adaptive continuun/discontinuum code*, in Clays in Natural end Engineered Barriers for Radioactive Waste Confinement. Tours 2nd International Meeting, March 14-18, 2005.

Hazzard J. F., Young R. P., Maxwell (2000). *Micromechanical modelling of cracking and failure in brittle rocks*. Journal of Geophysical Research, Vol 105, 37555-37569.

Hazzard J. F., Collins D. S., Pettit W. S., Young R. P. (2002). *Simulation of unstable fault slip in granite using a bonded particle model*. Pure and Applied Geophysics 159, 221-245.

Hazzard J. F., Young R. P. (2002b). *Moment tensors and micromechanical models*. Tectonophysics, 356(1-3), 181-197.

Itasca Consulting Group. (1999) *PFC2D (Particle Flow Code in 2 dimensions)*. Minneapolis, Minessota: Itasca Consulting Group, Inc.

Itasca Consulting Group. (1999) *FLAC (Fast Lagrangian Analysis of Continua)*. Minneapolis, Minessota: Itasca Consulting Group, Inc.

Johnston, J. C., Einstein, M. H., 1990, *A survey of mining associated seismicity*; Proc 2nd Int Symp Rockbursts and Seismicity in Mines, Minneapolis, Fairhurst (ed), Rotterdam:, A.A. Balkema, 121-127.

Kulatilake P., Malama B., Wang J. (2001) *Physical and particle flow modelling of jointed rock block behavior under uniaxial loading*, International Journal of Rock Mechanics and Mining Sciences 38, 641-657.

Mendecki, A. J., van Aswegen, G., Mountfort, P., 1999 *A guide to routine seismic monitoring in mines*, in A Handbook on Rock Engineering Practice for Tabular Hard Rock Mines, Jager and Ryder (eds) SiMRAC, Cape Town, South Africa.

Potyondy D, Cundall P. (2004) *A bonded particle model for rock*. International Journal of Rock Mechanics and Mining Sciences, 41(8), 1329-1364.